Ultralow Noise BiFET Op Amp

AD743

FEATURES

ULTRALOW NOISE PERFORMANCE
2.9 nV/√Hz at 10 kHz
0.38 μV p-p, 0.1 Hz to 10 Hz
6.9 fA/√Hz Current Noise at 1 kHz

EXCELLENT DC PERFORMANCE
0.5 mV max Offset Voltage
250 pA max Input Bias Current
1000 V/mV min Open-Loop Gain

AC PERFORMANCE
2.8 V/μs Slew Rate
4.5 MHz Unity-Gain Bandwidth
THD = 0.0003% @ 1 kHz
Available in Tape and Reel in Accordance with EIA-481A Standard

APPLICATIONS
Sonar Preamplifiers
High Dynamic Range Filters (>140 dB)
Photodiode and IR Detector Amplifiers
Accelerometers

CONNECTION DIAGRAMS

8-Pin Plastic Mini-DIP (N) and 8-Pin Cerdip (Q) Packages

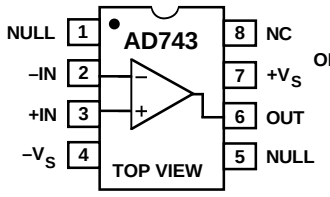

NC = NO CONNECT

16-Pin SOIC (R) Package

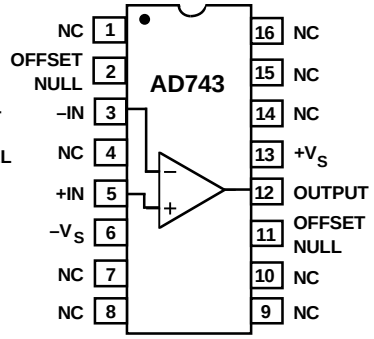

NC = NO CONNECT

PRODUCT DESCRIPTION

The AD743 is an ultralow noise precision, FET input, monolithic operational amplifier. It offers a combination of the ultralow voltage noise generally associated with bipolar input op amps and the very low input current of a FET-input device. Furthermore, the AD743 does not exhibit an output phase reversal when the negative common-mode voltage limit is exceeded.

The AD743's guaranteed, maximum input voltage noise of 4.0 nV/√Hz at 10 kHz is unsurpassed for a FET-input monolithic op amp, as is the maximum 1.0 μV p-p, 0.1 Hz to 10 Hz noise. The AD743 also has excellent dc performance with 250 pA maximum input bias current and 0.5 mV maximum offset voltage.

The AD743 is specifically designed for use as a preamp in capacitive sensors, such as ceramic hydrophones. It is available in five performance grades. The AD743J and AD743K are rated over the commercial temperature range of 0°C to +70°C. The AD743A and AD743B are rated over the industrial temperature range of –40°C to +85°C. The AD743S is rated over the military temperature range of –55°C to +125°C and is available processed to MIL-STD-883B, Rev. C.

The AD743 is available in 8-pin plastic mini-DIP, 8-pin cerdip, 16-pin SOIC, or in chip form.

PRODUCT HIGHLIGHTS

1. The low offset voltage and low input offset voltage drift of the AD743 coupled with its ultralow noise performance mean that the AD743 can be used for upgrading many applications now using bipolar amplifiers.
2. The combination of low voltage and low current noise make the AD743 ideal for charge sensitive applications such as accelerometers and hydrophones.
3. The low input offset voltage and low noise level of the AD743 provide >140 dB dynamic range.
4. The typical 10 kHz noise level of 2.9 nV/√Hz permits a three op amp instrumentation amplifier, using three AD743s, to be built which exhibits less than 4.2 nV/√Hz noise at 10 kHz and which has low input bias currents.

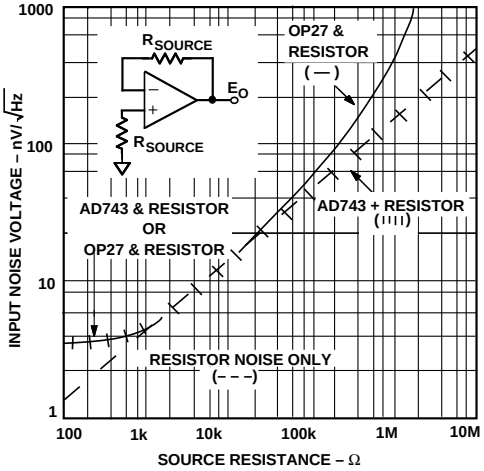

Input Noise Voltage vs. Source Resistance

REV. C

Information furnished by Analog Devices is believed to be accurate and reliable. However, no responsibility is assumed by Analog Devices for its use, nor for any infringements of patents or other rights of third parties which may result from its use. No license is granted by implication or otherwise under any patent or patent rights of Analog Devices.

One Technology Way, P.O. Box 9106, Norwood, MA 02062-9106, U.S.A.
Tel: 617/329-4700 **Fax: 617/326-8703**

AD743–SPECIFICATIONS (@ +25°C and ±15 V dc, unless otherwise noted)

Model	Conditions	AD743J Min	AD743J Typ	AD743J Max	AD743K/B Min	AD743K/B Typ	AD743K/B Max	AD743S Min	AD743S Typ	AD743S Max	Units
INPUT OFFSET VOLTAGE[1]											
Initial Offset			0.25	1.0/0.8		0.1	0.5/0.25		0.25	1.0	mV
Initial Offset	T_{MIN} to T_{MAX}			1.5			1.0/0.50			2.0	mV
vs. Temp.	T_{MIN} to T_{MAX}		2			1			2		µV/°C
vs. Supply (PSRR)	12 V to 18 V[2]	90	96		100	106		90	96		dB
vs. Supply (PSRR)	T_{MIN} to T_{MAX}	88			98	100		88			dB
INPUT BIAS CURRENT[3]											
Either Input	V_{CM} = 0 V		150	400		150	250		150	400	pA
Either Input @ T_{MAX}	V_{CM} = 0 V			8.8/25.6			5.5/16			413	nA
Either Input	V_{CM} = +10 V		250	600		250	400		300	600	pA
Either Input, V_S = ±5 V	V_{CM} = 0 V		30	200		30	125		30	200	pA
INPUT OFFSET CURRENT	V_{CM} = 0 V		40	150		30	75		40	150	pA
Offset Current @ T_{MAX}	V_{CM} = 0 V			2.2/6.4			1.1/3.2			102	nA
FREQUENCY RESPONSE											
Gain BW, Small Signal	G = –1		4.5			4.5			4.5		MHz
Full Power Response	V_O = 20 V p-p		25			25			25		kHz
Slew Rate, Unity Gain	G = –1		2.8			2.8			2.8		V/µs
Settling Time to 0.01%			6			6			6		µs
Total Harmonic Distortion[4] (Figure 16)	f = 1 kHz G = –1		0.0003			0.0003			0.0003		%
INPUT IMPEDANCE											
Differential			1×10^{10}‖20			1×10^{10}‖20			1×10^{10}‖20		Ω‖pF
Common Mode			3×10^{11}‖18			3×10^{11}‖18			3×10^{11}‖18		Ω‖pF
INPUT VOLTAGE RANGE											
Differential[5]			±20			±20			±20		V
Common-Mode Voltage			+13.3, –10.7			+13.3, –10.7			+13.3, –10.7		V
Over Max Operating Range[6]		–10		+12	–10		+12	–10		+12	V
Common-Mode Rejection Ratio	V_{CM} = ±10 V	80	95		90	102		80	95		dB
	T_{MIN} to T_{MAX}	78			88			78			dB
INPUT VOLTAGE NOISE	0.1 Hz to 10 Hz		0.38			0.38	1.0		0.38		µV p-p
	f = 10 Hz		5.5			5.5	10.0		5.5		nV/√Hz
	f = 100 Hz		3.6			3.6	6.0		3.6		nV/√Hz
	f = 1 kHz		3.2	5.0		3.2	5.0		3.2	5.0	nV/√Hz
	f = 10 kHz		2.9	4.0		2.9	4.0		2.9	4.0	nV/√Hz
INPUT CURRENT NOISE	f = 1 kHz		6.9			6.9			6.9		fA/√Hz
OPEN LOOP GAIN	V_O = ±10 V										
	R_{LOAD} ≥ 2 kΩ	1000	4000		2000	4000		1000	4000		V/mV
	T_{MIN} to T_{MAX}	800			1800			800			V/mV
	R_{LOAD} = 600 Ω		1200			1200			1200		V/mV
OUTPUT CHARACTERISTICS											
Voltage	R_{LOAD} ≥ 600 Ω	+13, –12			+13, –12			+13, –12			V
	R_{LOAD} ≥ 600 Ω		+13.6, –12.6			+13.6, –12.6			+13.6, –12.6		V
	T_{MIN} to T_{MAX}	+12, –10			+12, –10			+12, –10			V
	R_{LOAD} ≥ 2 kΩ	±12	+13.8, –13.1		±12	+13.8, –13.1		±12	+13.8, –13.1		V
Current	Short Circuit	20	40		20	40		20	40		mA
POWER SUPPLY											
Rated Performance			±15			±15			±15		V
Operating Range		±4.8		±18	±4.8		±18	±4.8		±18	V
Quiescent Current			8.1	10.0		8.1	10.0		8.1	10.0	mA
TRANSISTOR COUNT	# of Transistors		50			50			50		

NOTES

[1]Input offset voltage specifications are guaranteed after 5 minutes of operation at T_A = +25°C.

[2]Test conditions: $+V_S$ = 15 V, $–V_S$ = 12 V to 18 V and $+V_S$ = 12 V to +18 V, $–V_S$ = 15 V.

[3]Bias current specifications are guaranteed maximum at either input after 5 minutes of operation at T_A = +25°C. For higher temperature, the current doubles every 10°C.

[4]Gain = –1, R_L = 2 kΩ, C_L = 10 pF.

[5]Defined as voltage between inputs, such that neither exceeds ±10 V from common.

[6]Thc AD743 does not exhibit an output phase reversal when the negative common-mode limit is exceeded.

All min and max specifications are guaranteed.

Specifications subject to change without notice.

ABSOLUTE MAXIMUM RATINGS[1]

Supply Voltage . . . . . ±18 V
Internal Power Dissipation[2]
Input Voltage . . . . . $\pm V_S$
Output Short Circuit Duration . . . . . Indefinite
Differential Input Voltage . . . . . $+V_S$ and $-V_S$
Storage Temperature Range (Q) . . . . . –65°C to +150°C
Storage Temperature Range (N, R) . . . . . –65°C to +125°C
Operating Temperature Range
AD743J/K . . . . . 0°C to +70°C
AD743A/B . . . . . –40°C to +85°C
AD743S . . . . . –55°C to +125°C
Lead Temperature Range (Soldering 60 seconds) . . . . . 300°C

NOTES

[1]Stresses above those listed under "Absolute Maximum Ratings" may cause permanent damage to the device. This is a stress rating only and functional operation of the device at these or any other conditions above those indicated in the operational section of this specification is not implied. Exposure to absolute maximum rating conditions for extended periods may affect device reliability.

[2]8-pin plastic package: θ_{JA} = 100°C/Watt, θ_{JC} = 50°C/Watt
8-pin cerdip package: θ_{JA} = 110°C/Watt, θ_{JC} = 30°C/Watt
16-pin plastic SOIC package: θ_{JA} = 100°C/Watt, θ_{JC} = 30°C/Watt

ESD SUSCEPTIBILITY

An ESD classification per method 3015.6 of MIL-STD-883C has been performed on the AD743. The AD743 is a class 1 device, passing at 1000 V and failing at 1500 V on null pins 1 and 5, when tested, using an IMCS 5000 automated ESD tester. Pins other than null pins fail at greater than 2500 V.

ORDERING GUIDE

Model	Temperature Range	Package Option*
AD743JN	0°C to +70°C	N-8
AD743KN	0°C to +70°C	N-8
AD743JR-16	0°C to +70°C	R-16
AD743KR-16	0°C to +70°C	R-16
AD743BQ	–40°C to +85°C	Q-8
AD743SQ/883B	–55°C to +125°C	Q-8
AD743JR-16-REEL	0°C to +70°C	Tape & Reel
AD743KR-16-REEL	0°C to +70°C	Tape & Reel

*N = Plastic DIP; R = Small Outline IC; Q = Cerdip.

METALIZATION PHOTOGRAPH

Contact factory for latest dimensions.
Dimensions shown in inches and (mm).

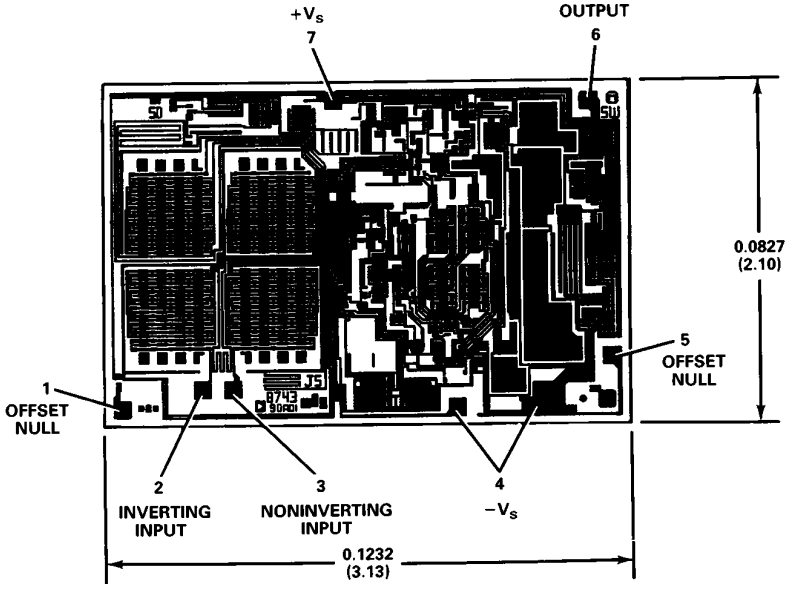

AD743–Typical Characteristics (@ +25°C, V_S = +15 V)

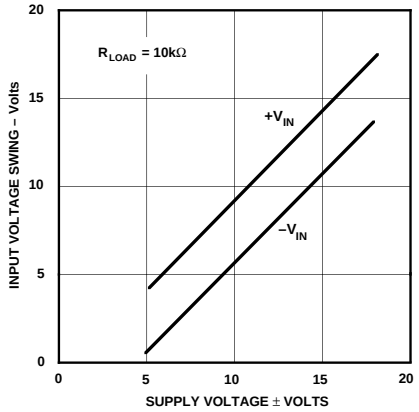

Figure 1. Input Voltage Swing vs. Supply Voltage

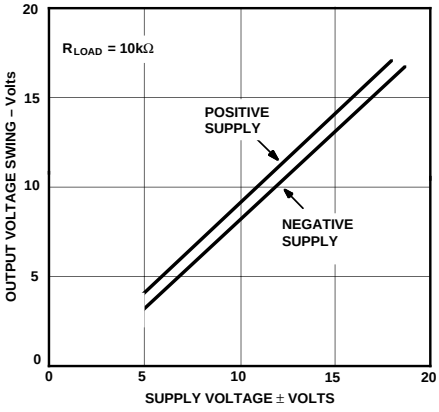

Figure 2. Output Voltage Swing vs. Supply Voltage

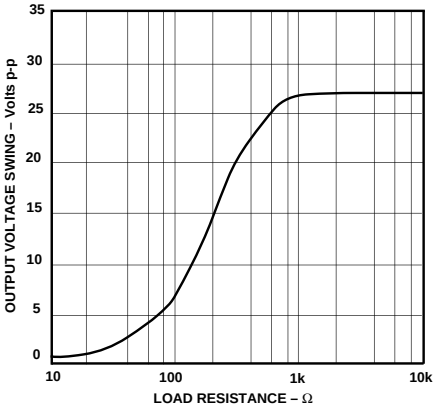

Figure 3. Output Voltage Swing vs. Load Resistance

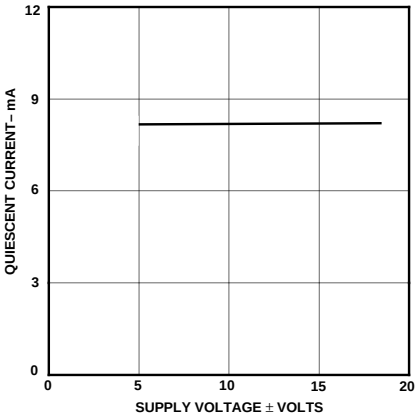

Figure 4. Quiescent Current vs. Supply Voltage

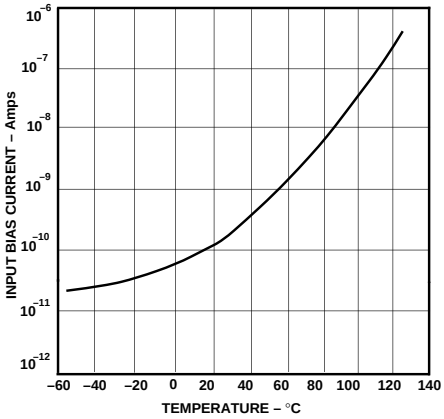

Figure 5. Input Bias Current vs. Temperature

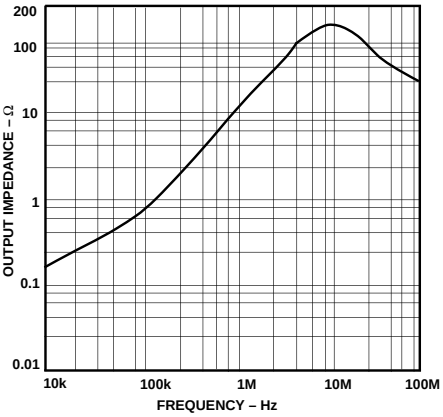

Figure 6. Output Impedance vs. Frequency (Closed Loop Gain = –1)

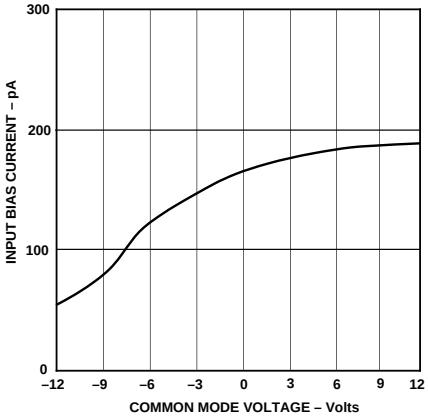

Figure 7. Input Bias Current vs. Common-Mode Voltage

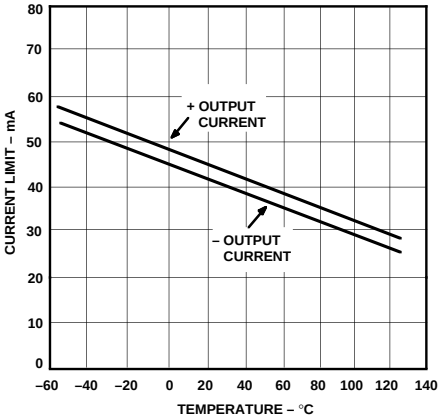

Figure 8. Short Circuit Current Limit vs. Temperature

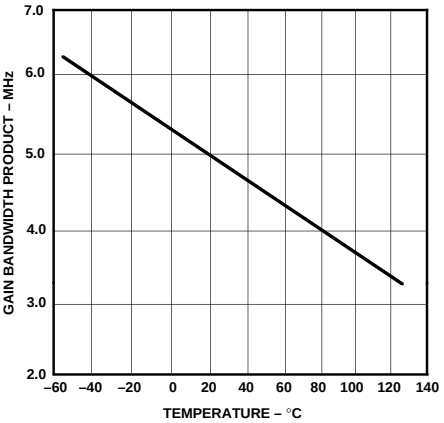

Figure 9. Gain Bandwidth Product vs. Temperature

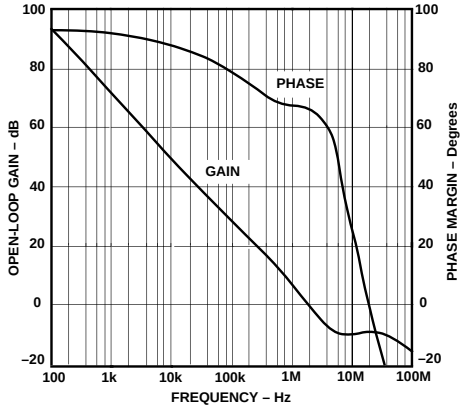

Figure 10. Open-Loop Gain and Phase vs. Frequency

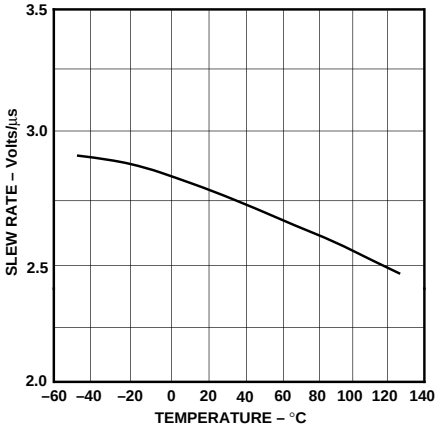

Figure 11. Slew Rate vs. Temperature (Gain = –1)

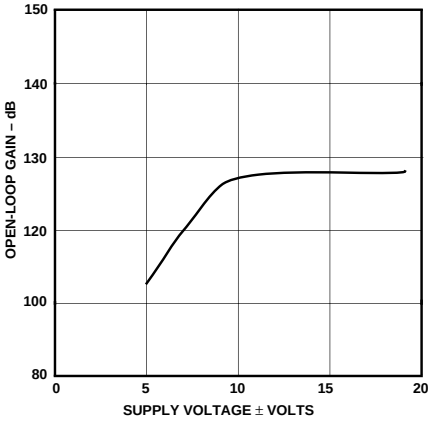

Figure 12. Open-Loop Gain vs. Supply Voltage, R_{LOAD} = 2K

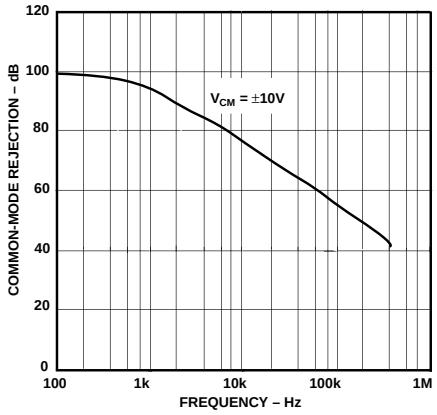

Figure 13. Common-Mode Rejection vs. Frequency

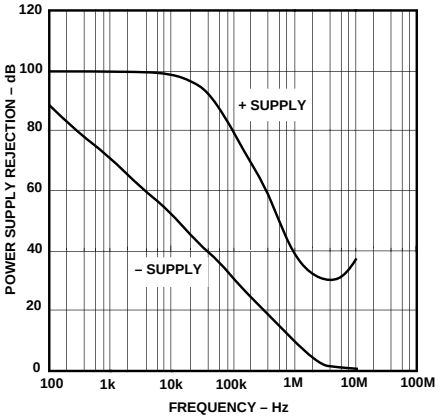

Figure 14. Power Supply Rejection vs. Frequency

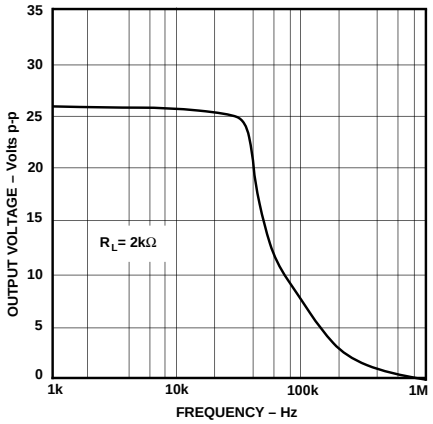

Figure 15. Large Signal Frequency Response

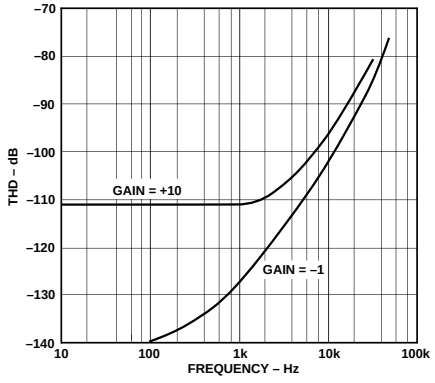

Figure 16. Total Harmonic Distortion vs. Frequency

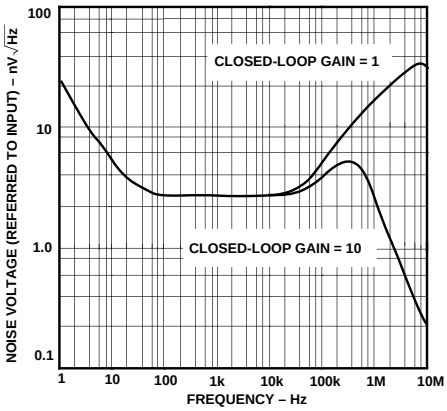

Figure 17. Input Noise Voltage Spectral Density

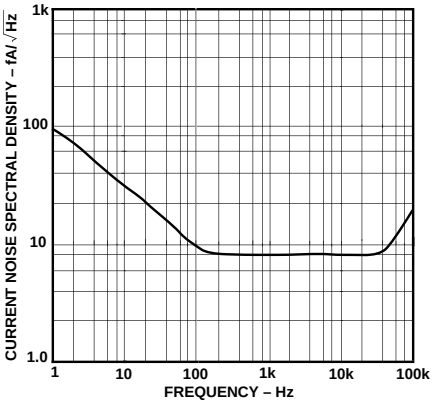

Figure 18. Input Noise Current Spectral Density

AD743–Typical Characteristics (@ +25°C, V_S = +15 V)

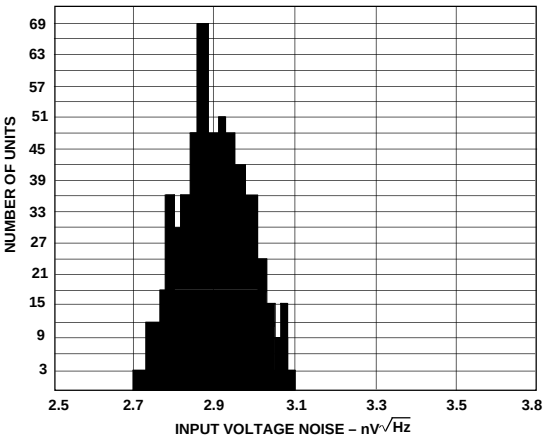

Figure 19. Typical Noise Distribution @ 10 kHz (602 Units)

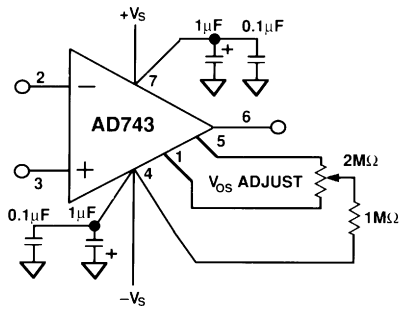

Figure 20. Offset Null Configuration

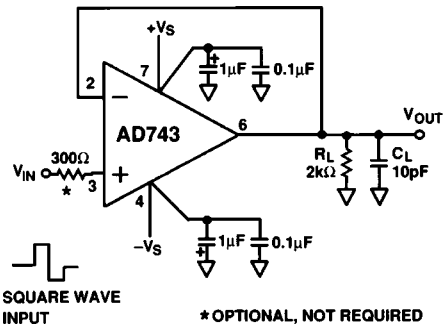

Figure 21. Unity-Gain Follower

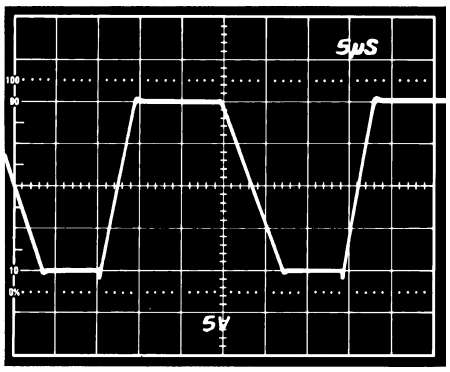

Figure 22a. Unity-Gain Follower Large Signal Pulse Response

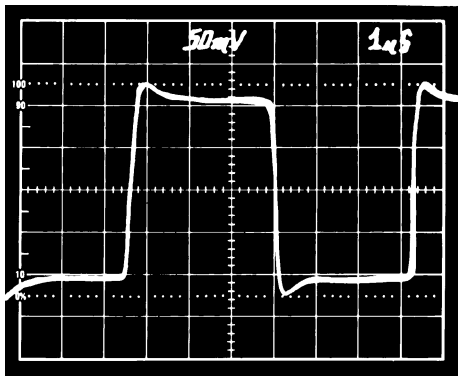

Figure 22b. Unity-Gain Follower Small Signal Pulse Response

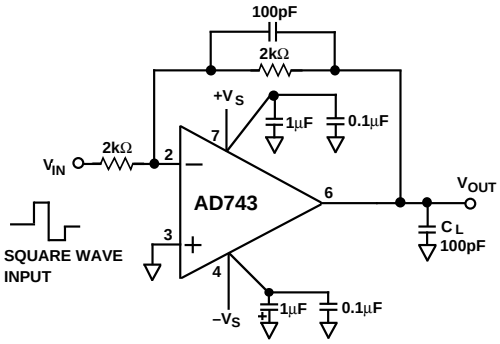

Figure 23a. Unity-Gain Inverter

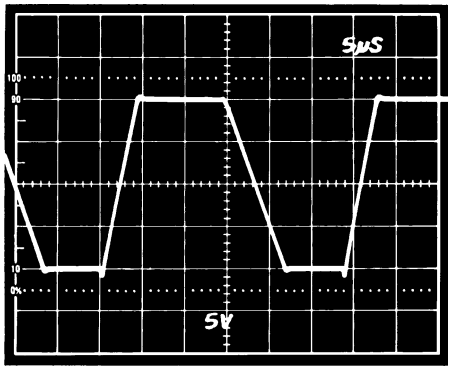

Figure 23b. Unity-Gain Inverter Large Signal Pulse Response

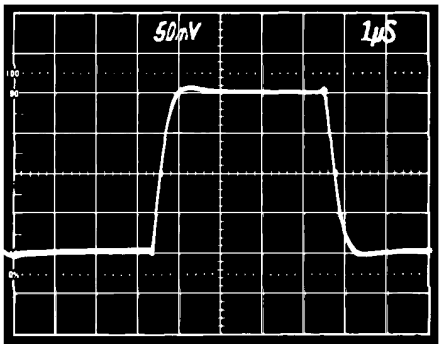

Figure 23c. Unity-Gain Inverter Small Signal Pulse Response

OP AMP PERFORMANCE: JFET VS. BIPOLAR

The AD743 is the first monolithic JFET op amp to offer the low input voltage noise of an industry-standard bipolar op amp without its inherent input current errors. This is demonstrated in Figure 24, which compares input voltage noise vs. input source resistance of the OP27 and the AD743 op amps. From this figure, it is clear that at high source impedance the low current noise of the AD743 also provides lower total noise. It is also important to note that with the AD743 this noise reduction extends all the way down to low source impedances. The lower dc current errors of the AD743 also reduce errors due to offset and drift at high source impedances (Figure 25).

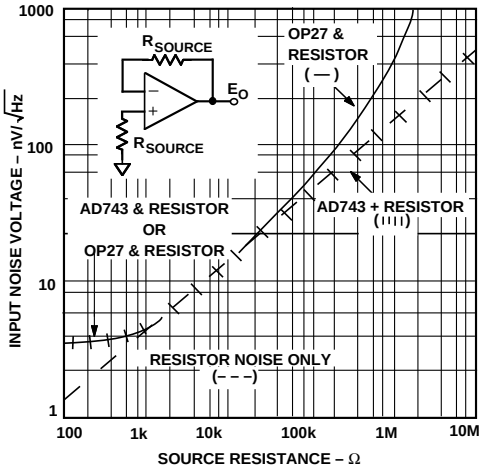

Figure 24. Total Input Noise Spectral Density @ 1 kHz vs. Source Resistance

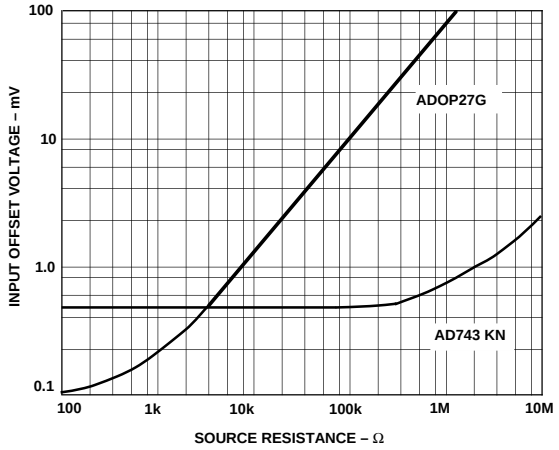

Figure 25. Input Offset Voltage vs. Source Resistance

DESIGNING CIRCUITS FOR LOW NOISE

An op amp's input voltage noise performance is typicaly divided into two regions: flatband and low frequency noise. The AD743 offers excellent performance with respect to both. The figure of 2.9 nV/$\sqrt{\text{Hz}}$ @ 10 kHz is excellent for JFET input amplifier. The 0.1 Hz to 10 Hz noise is typically 0.38 μV p-p. The user should pay careful attention to several design details in order to optimize low frequency noise performance. Random air currents can generate varying thermocouple voltages that appear as low frequency noise: therefore sensitive circuitry should be well shielded from air flow. Keeping absolute chip temperature low also reduces low frequency noise in two ways: first, the low frequency noise is strongly dependent on the ambient temperature and increases above +25°C. Secondly, since the gradient of temperature from the IC package to ambient is greater, the noise generated by random air currents, as previously mentioned, will be larger in magnitude. Chip temperature can be reduced both by operation at reduced supply voltages and by the use of a suitable clip-on heat sink, if possible.

Low frequency current noise can be computed from the magnitude of the dc bias current ($\tilde{I}_n = \sqrt{2qI_B\Delta f}$) and increases below approximately 100 Hz with a 1/f power spectral density. For the AD743 the typical value of current noise is 6.9 fA/$\sqrt{\text{Hz}}$ at 1 kHz. Using the formula, $\tilde{I}_n = \sqrt{4kT/R\Delta f}$, to compute the Johnson noise of a resistor, expressed as a current, one can see that the current noise of the AD743 is equivalent to that of a $3.45 \times 10^8\ \Omega$ source resistance.

At high frequencies, the current noise of a FET increases proportionately to frequency. This noise is due to the "real" part of the gate input impedance, which decreases with frequency. This noise component usually is not important, since the voltage noise of the amplifier impressed upon its input capacitance is an apparent current noise of approximately the same magnitude.

In any FET input amplifier, the current noise of the internal bias circuitry can be coupled externally via the gate-to-source capacitances and appears as input current noise. This noise is totally correlated at the inputs, so source impedance matching will tend to cancel out its effect. Both input resistance and input capacitance should be balanced whenever dealing with source capacitances of less than 300 pF in value.

LOW NOISE CHARGE AMPLIFIERS

As stated, the AD743 provides both low voltage and low current noise. This combination makes this device particularly suitable in applications requiring very high charge sensitivity, such as capacitive accelerometers and hydrophones. When dealing with a high source capacitance, it is useful to consider the total input charge uncertainty as a measure of system noise.

Charge (Q) is related to voltage and current by the simply stated fundamental relationships:

$$Q = CV \text{ and } I = \frac{dQ}{dt}$$

As shown, voltage, current and charge noise can all be directly related. The change in open circuit voltage (ΔV) on a capacitor will equal the combination of the change in charge (ΔQ/C) and the change in capacitance with a built in charge (Q/ΔC).

Figures 26 and 27 show two ways to buffer and amplify the output of a charge output transducer. Both require using an amplifier which has a very high input impedance, such as the AD743. Figure 26 shows a model of a charge amplifier circuit. Here, amplification depends on the principle of conservation of charge at the input of amplifier A1, which requires that the charge on capacitor C_S be transferred to capacitor C_F, thus yielding an output voltage of $\Delta Q/C_F$. The amplifiers input voltage noise will appear at the output amplified by the noise gain $(1 + (C_S/C_F))$ of the circuit.

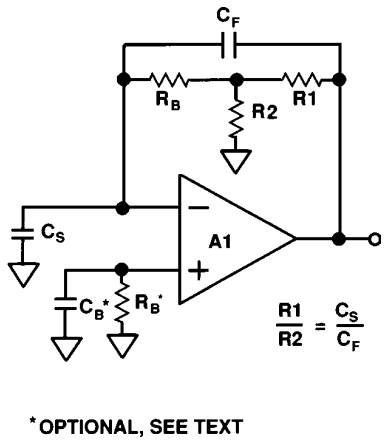

Figure 26. A Charge Amplifier Circuit

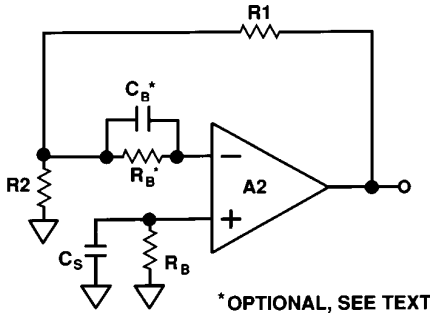

Figure 27. Model for a High Z Follower with Gain

The second circuit, Figure 27, is simply a high impedance follower with gain. Here the noise gain (1 + (R1/R2)) is the same as the gain from the transducer to the output. Resistor R_B, in both circuits, is required as a dc bias current return.

There are three important sources of noise in these circuits. Amplifiers A1 and A2 contribute both voltage and current noise, while resistor R_B contributes a current noise of:

$$\tilde{N} = \sqrt{4k\frac{T}{R_B}\Delta f}$$

where:

k = Boltzman's Constant = 1.381 x 10^{-23} Joules/Kelvin

T = Absolute Temperature, Kelvin (0°C = +273.2 Kelvin)

Δf = Bandwidth – in Hz (Assuming an Ideal "Brick Wall" Filter)

This must be root-sum-squared with the amplifier's own current noise.

Figure 28 shows that these two circuits have an identical frequency response and the same noise performance (provided that C_S/C_F = R1/ R2). One feature of the first circuit is that a "T" network is used to increase the effective resistance of R_B and improve the low frequency cutoff point by the same factor.

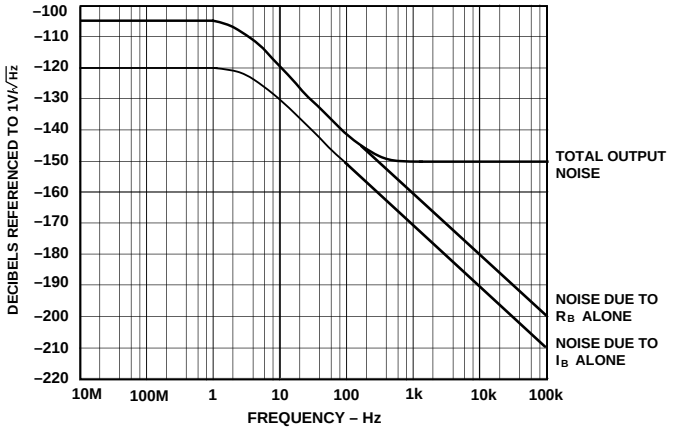

Figure 28. Noise at the Outputs of the Circuits of Figures 26 and 27. Gain = 10, C_S = 3000 pF, R_B = 22 MΩ

However, this does not change the noise contribution of R_B which, in this example, dominates at low frequencies. The graph of Figure 29 shows how to select an R_B large enough to minimize this resistor's contribution to overall circuit noise. When the equivalent current noise of R_B ($(\sqrt{4kT})/R$) equals the noise of I_B ($\sqrt{2qI_B}$), there is diminishing return in making R_B larger.

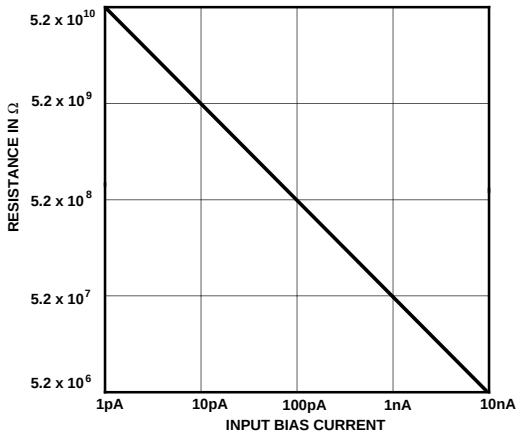

Figure 29. Graph of Resistance vs. Input Bias Current where the Equivalent Noise $\sqrt{4kT/R}$, Equals the Noise of the Bias Current $\sqrt{2qI_B}$

To maximize dc performance over temperature, the source resistances should be balanced on each input of the amplifier. This is represented by the optional resistor R_B in Figures 26 and 27. As previously mentioned, for best noise performance care should be taken to also balance the source capacitance designated by C_B. The value for C_B in Figure 26 would be equal to C_S, in Figure 27. At values of C_B over 300 pF, there is a diminishing impact on noise; capacitor C_B can then be simply a large bypass of 0.01 µF or greater.

HOW CHIP PACKAGE TYPE AND POWER DISSIPATION AFFECT INPUT BIAS CURRENT

As with all JFET input amplifiers, the input bias current of the AD743 is a direct function of device junction temperature, I_B approximately doubling every 10°C. Figure 30 shows the relationship between bias current and junction temperature for the AD743. This graph shows that lowering the junction temperature will dramatically improve I_B.

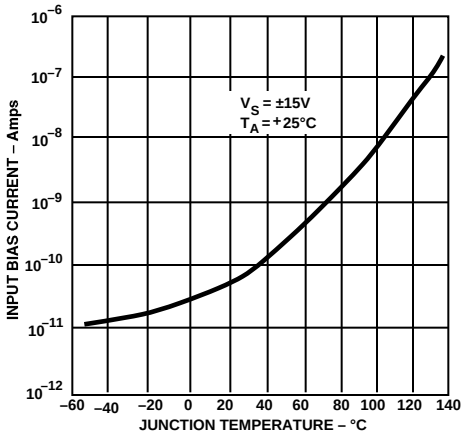

Figure 30. Input Bias Current vs. Junction Temperature

The dc thermal properties of an IC can be closely approximated by using the simple model of Figure 31 where current represents power dissipation, voltage represents temperature, and resistors represent thermal resistance (θ in °C/Watt).

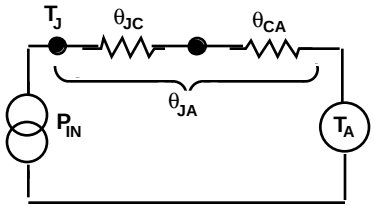

WHERE:
P_{IN} = DEVICE DISSIPATION
T_A = AMBIENT TEMPERATURE
T_J = JUNCTION TEMPERATURE
θ_{JC} = THERMAL RESISTANCE – JUNCTION TO CASE
θ_{CA} = THERMAL RESISTANCE – CASE TO AMBIENT

Figure 31. A Device Thermal Model

From this model $T_J = T_A + \theta_{JA}$ Pin. Therefore, I_B can be determined in a particular application by using Figure 30 together with the published data for θ_{JA} and power dissipation. The user can modify θ_{JA} by use of an appropriate clip-on heat sink such as the Aavid #5801. θ_{JA} is also a variable when using the AD743 in chip form. Figure 32 shows bias current vs. supply voltage with θ_{JA} as the third variable. This graph can be used to predict bias current after θ_{JA} has been computed. Again bias current will double for every 10°C. The designer using the AD743 in chip form (Figure 33) must also be concerned with both θ_{JC} and θ_{CA}, since θ_{JC} can be affected by the type of die mount technology used.

Typically, θ_{JC}'s will be in the 3°C to 5°C/watt range; therefore, for normal packages, this small power dissipation level may be ignored. But, with a large hybrid substrate, θ_{JC} will dominate proportionately more of the total θ_{JA}.

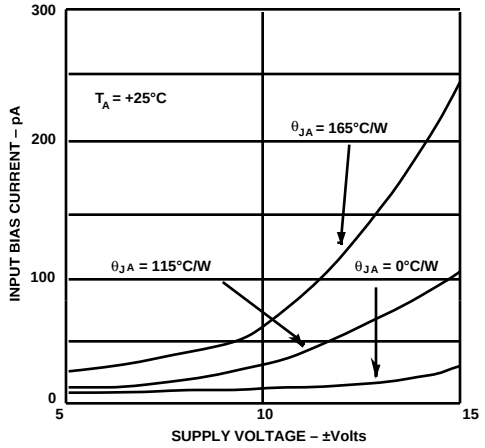

Figure 32. Input Bias Current vs. Supply Voltage for Various Values of θ_{JA}

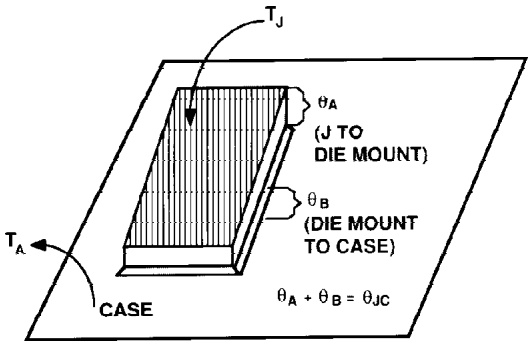

Figure 33. A Breakdown of Various Package Thermal Resistances

REDUCED POWER SUPPLY OPERATION FOR LOWER I_B

Reduced power supply operation lowers I_B in two ways: first, by lowering both the total power dissipation and second, by reducing the basic gate-to-junction leakage (Figure 32). Figure 34 shows a 40 dB gain piezoelectric transducer amplifier, which operates without an ac coupling capacitor, over the –40°C to +85°C temperature range. If the optional coupling capacitor is used, this circuit will operate over the entire –55°C to +125°C military temperature range.

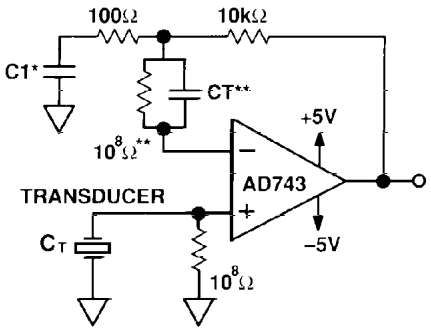

Figure 34. A Piezoelectric Transducer

AN INPUT-IMPEDANCE-COMPENSATED, SALLEN-KEY FILTER

The simple high pass filter of Figure 35 has an important source of error which is often overlooked. Even 5 pF of input capacitance in amplifier "A" will contribute an additional 1% of passband amplitude error, as well as distortion, proportional to the C/V characteristics of the input junction capacitance. The addition of the network designated "Z" will balance the source impedance–as seen by "A"–and thus eliminate these errors.

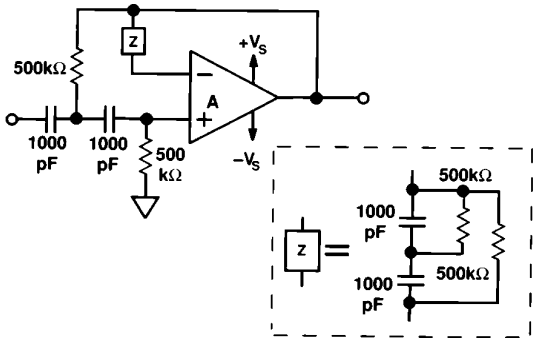

Figure 35. An Input Impedance Compensated Sallen-Key Filter

TWO HIGH PERFORMANCE ACCELEROMETER AMPLIFIERS

Two of the most popular charge-out transducers are hydrophones and accelerometers. Precision accelerometers are typically calibrated for a charge output (pC/g).* Figures 36a and 36b show two ways in which to configure the AD743 as a low noise charge amplifier for use with a wide variety of piezoelectric accelerometers. The input sensitivity of these circuits will be determined by the value of capacitor C1 and is equal to:

$$\Delta V_{OUT} = \frac{\Delta Q_{OUT}}{C1}$$

The ratio of capacitor C1 to the internal capacitance (C_T) of the transducer determines the noise gain of this circuit ($1 + C_T/C1$). The amplifiers voltage noise will appear at its output amplified by this amount. The low frequency bandwidth of these circuits will be dependent on the value of resistor R1. If a "T" network is used, the effective value is: R1 (1 + R2/R3).

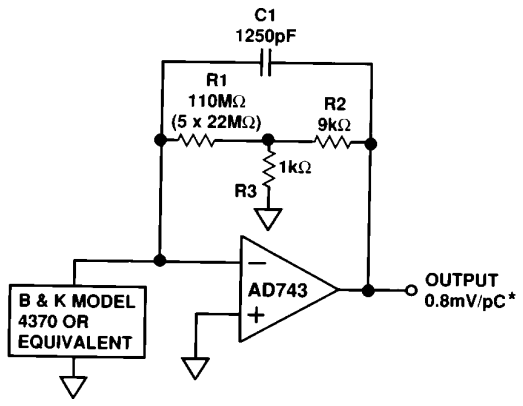

Figure 36a. A Basic Accelerometer Circuit

*pC = Picocoulombs
g = Earth's Gravitational Constant

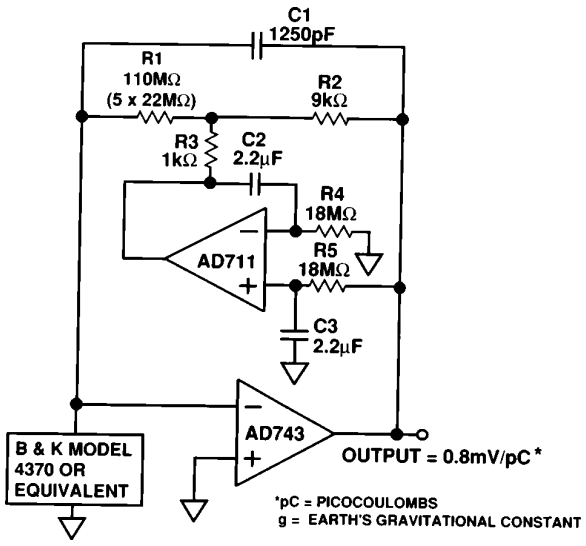

Figure 36b. An Accelerometer Circuit Employing a DC Servo Amplifier

A dc servo-loop (Figure 36b) can be used to assure a dc output which is <10 mV, without the need for a large compensating resistor when dealing with bias currents as large as 100 nA. For optimal low frequency performance, the time constant of the servo loop (R4C2 = R5C3) should be:

$$Time\ Constant \geq 10\,R1\left(1+\frac{R2}{R3}\right)C1$$

A LOW NOISE HYDROPHONE AMPLIFIER

Hydrophones are usually calibrated in the voltage-out mode. The circuits of Figures 37a and 37b can be used to amplify the output of a typical hydrophone. Figure 37a shows a typical dc coupled circuit. The optional resistor and capacitor serve to counteract the dc offset caused by bias currents flowing through resistor R1. Figure 37b, a variation of the original circuit, has a low frequency cutoff determined by an RC time constant equal to:

$$Time\ Constant = \frac{1}{2\pi \times C_C \times 100\Omega}$$

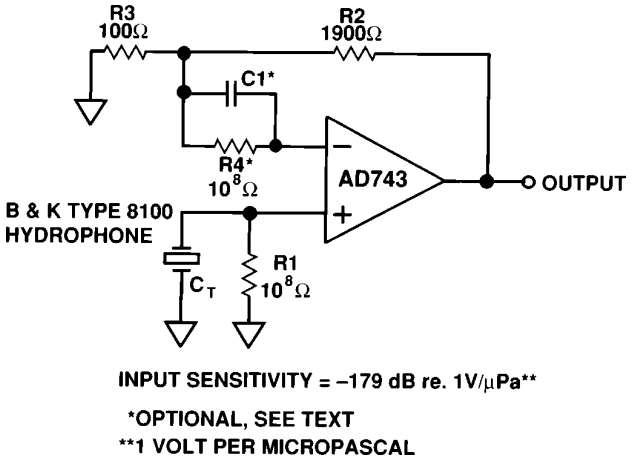

Figure 37a. A Basic Hydrophone Amplifier

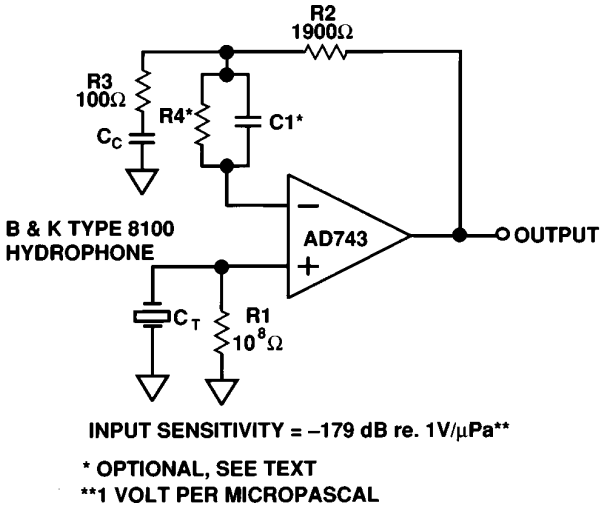

Figure 37b. An AC-Coupled, Low Noise Hydrophone Amplifier

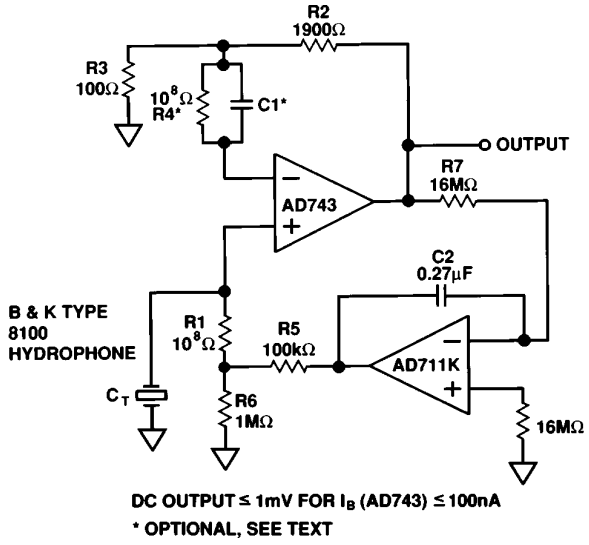

Figure 37c. A Hydrophone Amplifier Incorporating a DC Servo Loop

Where the dc gain is 1 and the gain above the low frequency cutoff ($1/(2\pi C_C(100\ \Omega))$) is the same as the circuit of Figure 37a. The circuit of Figure 37c uses a dc servo loop to keep the dc output at 0 V and to maintain full dynamic range for I_B's up to 100 nA. The time constant of R7 and C2 should be larger than that of R1 and C_T for a smooth low frequency response.

The transducer shown has a source capacitance of 7500 pF. For smaller transducer capacitances (≤300 pF), lowest noise can be achieved by adding a parallel RC network (R4 = R1, C1 = C_T) in series with the inverting input of the AD743.

BALANCING SOURCE IMPEDANCES

As mentioned previously, it is good practice to balance the source impedances (both resistive and reactive) as seen by the inputs of the AD743. Balancing the resistive components will optimize dc performance over temperature because balancing will mitigate the effects of any bias current errors. Balancing input capacitance will minimize ac response errors due to the amplifier's input capacitance and, as shown in Figure 38, noise performance will be optimized. Figure 39 shows the required external components for noninverting (A) and inverting (B) configurations.

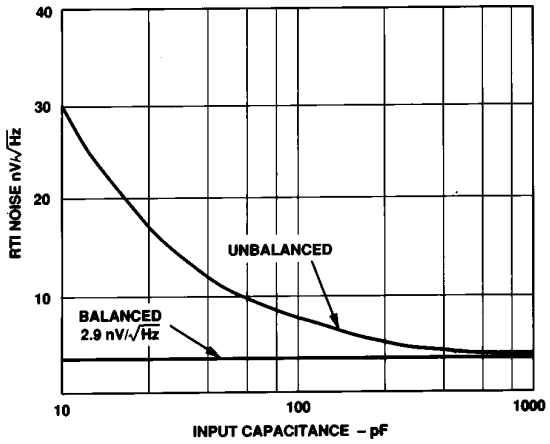

Figure 38. RTI Voltage Noise vs. Input Capacitance

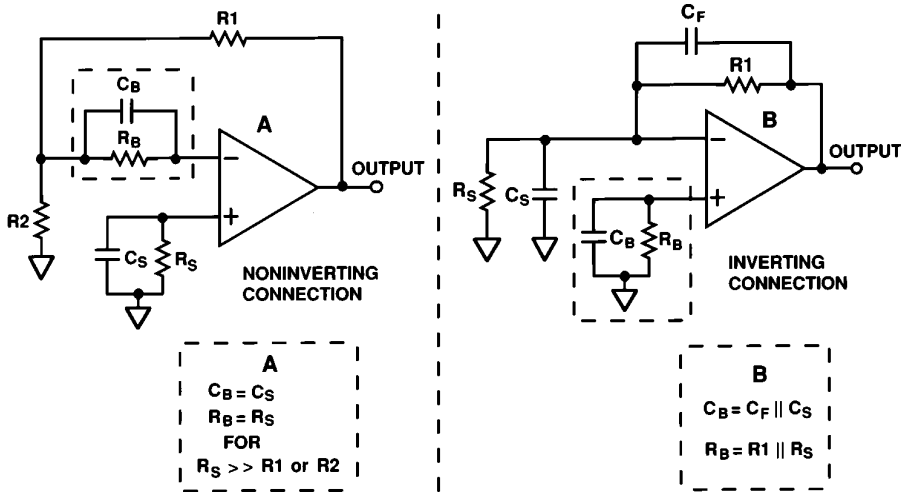

Figure 39. Optional External Components for Balancing Source Impedances

OUTLINE DIMENSIONS

Dimensions shown in inches and (mm).

8-Pin Plastic Mini-DIP (N)

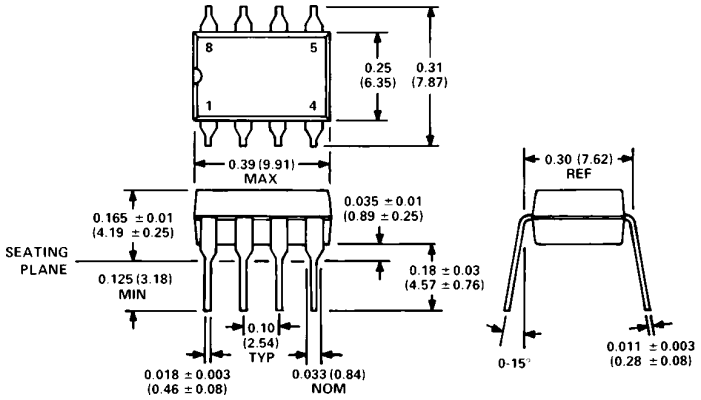

8-Pin Cerdip (Q) Packages

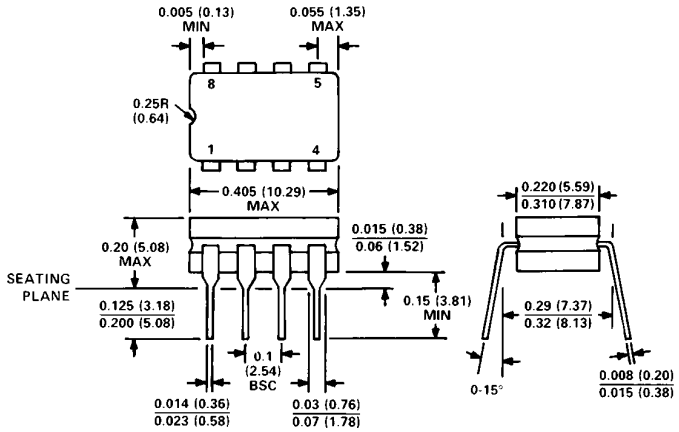

16-Pin SOIC (R) Package

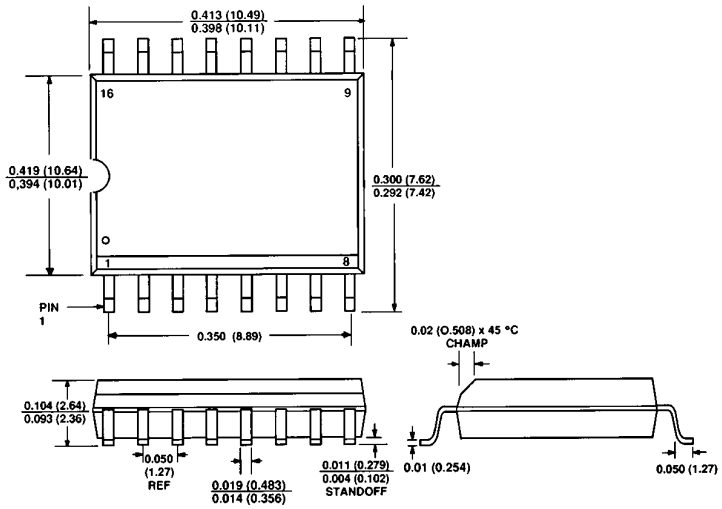

C1433–24–10/90

PRINTED IN U.S.A.